Catalysis Today 175 (2011) 164–170

Contents lists available at ScienceDirect

Catalysis Today

journal homepage: www.elsevier.com/locate/cattod

Low temperature selective catalytic reduction of NO and NO_2 with NH_3 over activated carbon-supported vanadium oxide catalyst

Xiang Gao*, Shaojun Liu, Yang Zhang, Xuesen Du, Zhongyang Luo, Kefa Cen

State Key Laboratory of Clean Energy Utilization, Zhejiang University, 38 Zheda Road, Hangzhou 310027, PR China

ARTICLE INFO

Article history:
Received 13 October 2010
Received in revised form 21 February 2011
Accepted 30 March 2011
Available online 7 May 2011

Keywords:
Selective catalytic reduction
Ammonia
V_2O_5/AC
Nitrogen dioxide
Ammonium nitrate

ABSTRACT

Selective catalytic reduction (SCR) of NO and NO_2 with ammonia was investigated over activated carbon-supported vanadium oxide (V_2O_5/AC) catalyst. The results show that high activity and selectivity could be achieved in wide range of temperatures and space velocities. NO_x conversion to N_2 increases with increasing NO_2/NO_x ratio, and the increase vanishes gradually with increasing temperature. An increase of NO_x conversion to N_2 from 26% to 94% can be achieved at a temperature as low as 150 °C without the formation of NH_4NO_3. The results of temperature programmed desorption (TPD) and infrared (IR) spectrometry experiments show that NH_4NO_3 could be deposited on the catalyst at 100 °C and decomposed to NH_3, N_2O, and NO around 130 °C. To explain the observed behaviors, AC involved NO_2-SCR process was proposed, in which NH_4NO_3 is reduced to N_2 by AC instead of NO. This process shows better reactivity at lower temperatures.

1. Introduction

Selective catalytic reduction (SCR) with ammonia or urea is an important technology for the elimination of NO_x emitted from stationary power stations and diesel engines. The stoichiometry of the main reaction is known as the “standard SCR”:

$$4NH_3+4NO+O_2 \rightarrow 4N_2+6H_2O \quad (1)$$

However, current commercial SCR catalysts such as V_2O_5/TiO_2 and V_2O_5–WO_3/TiO_2 have to be operated in the temperature range at 300–400 °C, resulting in complicated processes and higher costs. For this reason, a large amount of research has been conducted, and several processes have been proposed [1–5].

One of the most promising solutions is the use of a low temperature SCR catalyst, for which a large number of catalysts have been evaluated [6–10]. In these studies, a V_2O_5/AC catalyst was found to be very promising in much effective NO removal activity around 250 °C [8]. Another solution is the application of the so-called “fast SCR” reaction, which was observed as early as the 1980s [11]. The reaction is considerably faster than the “standard SCR” in the field of low temperatures, with stoichiometry:

$$2NH_3+NO+NO_2 \rightarrow 2N_2+3H_2O \quad (2)$$

With the recent development of the non-thermal plasma (NTP) catalytic process and the oxidation catalyst, which can be installed upstream of the SCR catalyst to achieve an effective conversion of NO to NO_2 [12,13], more attention has been paid to the “fast SCR” process. The benefit of the “fast SCR” was reported for SCR catalysts such as V_2O_5–WO_3–MnO_2/TiO_2 and Fe–ZSM5 [14–16]. Several works were focused on elucidating the mechanisms involved [17,18]. More recently, the present authors have investigated the mechanism of the “fast SCR” on V_2O_5 catalyst using quantum chemistry calculations. The results showed that NO_2 could readily reoxidize V^{4+}–OH to V^{5+}=O through two reaction routes [19].

However, to the best of our knowledge, NO_x reduction on activated carbon-based catalyst with the coexistence of NO and NO_2 in the feed gas has been scarcely reported. Since NO_2 can be adsorbed on carbon material to form nitrogen complexes [20–22], the SCR of NO and NO_2 on the activated carbon-based catalyst may be different from other catalysts reported for “fast SCR”. In the present study, the catalytic property of a V_2O_5/AC catalyst was studied for NO_x reduction with NH_3 in the temperatures between 100 °C and 300 °C. NO_2 temperature programmed desorption (TPD) experiments were performed to evaluate the adsorbed species. The effects of temperature, space velocity, and NO_2/NO_x ratio on NO_x reduction over V_2O_5/AC catalyst were then evaluated. As a product led to low N_2 selectivity of the SCR process, the formation, deposition, and decomposition of NH_4NO_3 were investigated with TPD experiment and infrared (IR) spectroscopy.

2. Experimental

2.1. Catalyst preparation

The activated carbon (AC) used was a commercial product from Tangshan Huaneng Technology Carbon Co., Ltd., China. The

---

* Corresponding author. Tel.: +86 571 87951335; fax: +86 571 87951616.
E-mail address: xgao1@zju.edu.cn (X. Gao).

0920-5861/$ – see front matter © 2011 Elsevier B.V. All rights reserved.
doi:10.1016/j.cattod.2011.03.058

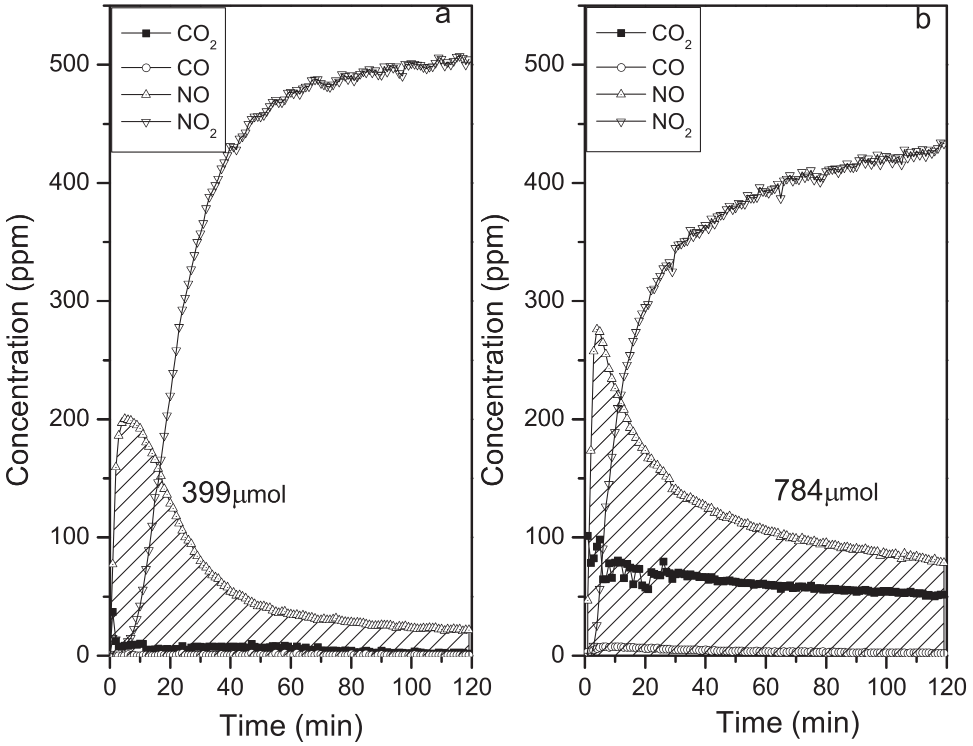

Fig. 1. Outlet concentrations of NO_2, NO, CO and CO_2 during the NO_2 adsorption. Reaction conditions: 500 ppm NO_2, 0% O_2, 0%H_2O, 72,000 L/(kg h) 50 °C for (a) and 150 °C for (b).

chemical composition and surface area have been described in detail elsewhere [23]. Before being used, the AC was oxidized with concentrated HNO_3 (3 mL/g AC) at 60 °C for 1 h, followed by washing with distilled water and drying overnight at 50 °C and then at 120 °C for 5 h. Vanadium oxide was supported on the AC by conventional pore volume impregnation with an aqueous solution of ammonium metavanadate in oxalic acid, followed by dried overnight at 50 °C and then at 120 °C for 5 h. The dried samples were calcinated in Ar for 5 h at 500 °C and then in air at 230 °C for 5 h. The vanadium loading on the catalyst used in this work (3 wt.%) was determined from the ammonium metavanadate concentration used for impregnation (confirmed by ICP analysis). The surface area of the resulting catalyst is 599 m^2/g and the average pore diameter is 3.21 nm.

2.2. Characterization of catalyst

Nitrogen adsorption–desorption isotherms were measured at −196 °C over a range of relative pressures on an Autosorb-1-C system (Quantachrome Instrument). The specific area was computed from isotherms using the Brunauer–Emmett–Teller (BET) method.

Infrared spectra were recorded on a Thermo Nicolet 380 FT-IR in a 400–4000 cm^{-1} wave number range. The samples were mixed with potassium bromide at a weight ratio of 1:100, ground and palletized, then scanned at a resolution of 4 cm^{-1}.

2.3. NO_2/NH_4NO_3-TPD

NO_2/NH_4NO_3-TPD experiments were performed in a 350 mm long quartz flow tube reactor (1 cm i.d.). In a typical experiment, 0.3g (NO_2) or 1g (NH_4NO_3) samples (30–60 mesh) were packed into the reactor within a temperature-controlled furnace. A thermocouple was inserted next to the catalyst to monitor the samples temperature. When treated with NO_2, the samples were pretreated in an Ar stream at 200 °C for 1 h and then cooled to the starting temperature (50 or 150 °C) in the same stream. The gas flow was then switched to the reactive gas mixture containing NO_2 (500 ppm by volume) in Ar. After adsorption for 2 h, the samples were purged successively with Ar for 1 h until the NO and NO_2 concentration in the effluent gas decreased to <15 ppm. A TPD test was run immediately at 10 °C/min to 900 °C to examine the adsorbed species. When treated with NH_4NO_3, the reactive gas mixture contained 450 ppm NO_2, 500 ppm NH_3, 5% O_2 and 3% H_2O. After reaction at 100 °C for 1 h, the samples were purged successively with Ar for 30 min until the outlet concentrations of NH_3 and NO decrease to less than 15 ppm. A TPD test was run immediately at 10 °C/min to 300 °C to examine the adsorbed species.

2.4. Activity and transient response tests

Catalytic activity tests were performed in the same reactor as the above experiment. In order to ensure the complete conversion of NO_x, a typical feeding gas composition was 450 ppm NO_x, 500 ppm NH_3, 5% O_2, and 3% H_2O. Ar was used as the balance gas. Water vapor was introduced by passing Ar through a heated gas-wash bottle containing deionized water. The H_2O content in the feed gas was controlled via the heating temperature. The gas lines were heated up to 100 °C in order to prevent water condensation. To avoid reaction between NO_2 and NH_3 prior to the catalyst bed, NH_3/Ar was fed directly into the reactor, bypassing the mixing chamber. The lines from the exit of the reactor to the gas analyzer were heated up to 180 °C in order to prevent the formation and deposition of NH_4NO_3. Different space velocities were obtained by changing the volume of catalyst used. To investigate the role of NO_2 in the SCR reaction on V_2O_5/AC, a transient response experiment was carried out by sequentially switching oxygen or water and changing the NO_2/NO_x ratio.

In both the NO_2/NH_4NO_3-TPD and the activity and transient response tests, a total flow rate of 1.2 L/min was used at 1 atm

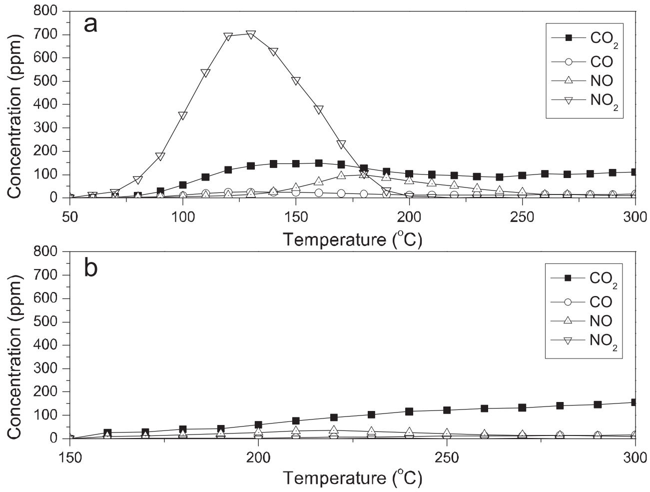

Fig. 2. Desorption spectra of the V_2O_5/AC catalyst after NO_2 adsorption for 120 min at (a) 50 °C and (b) 150 °C.

throughout the process. Each feeding gas flow rate was measured and controlled independently by a mass flow controller. Concentrations of NH_3, NO, NO_2, O_2, CO, CO_2, and N_2O were measured simultaneously using an on-line Fourier-transform IR spectrometer (GASMET, DX4000). The NO_x conversion to N_2 was obtained by the following equation:

$$NO_x \text{ conversion to } N_2 = \frac{[NO_x]_{\text{inlet}} - [NO_x]_{\text{outlet}}}{[NO_x]_{\text{inlet}}} \times 100\% \tag{3}$$

where $[NO_x]_{\text{inlet}}$ and $[NO_x]_{\text{outlet}}$ denote the total amount of NO_2, NO and N_2O at the inlet and outlet, respectively.

3. Results and discussion

3.1. NO_2-TPD

The results of the NO_2 adsorption experiment suggest that the adsorption of NO_2 and its reduction to NO occur simultaneously. The outlet NO and NO_2 reach steady state when the adsorption is saturated. The outlet NO_x is then balanced to the inlet NO_2 concentration. The results shown in Fig. 1 are very similar with those reported in [23], suggesting the reactions mainly occur over carbon surface. The steady-state NO and CO_2 concentrations in the NO_2 adsorption step at 150 °C were around 80 ppm and 50 ppm respectively, which are larger than the corresponding values of 50 °C. After 2 h of NO_2 adsorption, about 24% NO_2 was reduced by carbon at 150 °C, compared to 12% at 50 °C. This result reveals that the conversion of NO_2 to NO increases with increasing temperature. It is worth emphasizing that most of NO_2 was still in the feed gas at 150 °C. The outlet concentration of CO was <5 ppm. This is consistent with the results of the TPD experiments below, which show that the decomposition of oxygen complexes to CO is not obvious below 300 °C. The N_2O formation was also <5 ppm throughout this step, suggesting that a more severe reduction does not take place. The consumed and emitted oxygen concentrations can be calculated from the NO_2, NO, N_2O, CO_2, and CO concentrations. However, a balance cannot be achieved, confirming the formation of oxygen complexes on the catalyst.

A TPD test was performed after the adsorption and purge at 50 °C. The results are presented in Fig. 2a. Since the NO_2 and NO desorption is almost complete, we present the desorption spectra of NO, NO_2, CO, and CO_2 to 300 °C. A sharp desorption of NO_2 with a peak around 130 °C could be observed at first. Desorption of NO and CO_2 was then observed, whereas CO was presented only as a minor product. The different desorption peaks of NO and NO_2 suggest the variety of the adsorbed nitrogen complexes, which have different chemical natures and thermal stabilities. After the desorption peaks, the emission of NO and NO_2 decreased and almost vanished at 300 °C, suggesting that most of the nitrogen containing species created during exposure to NO_2 are no longer stable above this temperature. This is consistent with the previous reports of the NO_2 adsorption on carbon material [20–24]. Fig. 2b shows the results of the TPD experiment after adsorption at 150 °C. The emission peaks of NO_2 disappeared, indicating that nitrogen complexes are nearly not retained on the catalyst at this temperature. The emission of CO_2 after 230 °C is similar to that in Fig. 1a. This result can be attributed to that the oxygen complexes are still produced by NO_2 reduction at 150 °C, and then decomposed to CO_2 with increasing temperature.

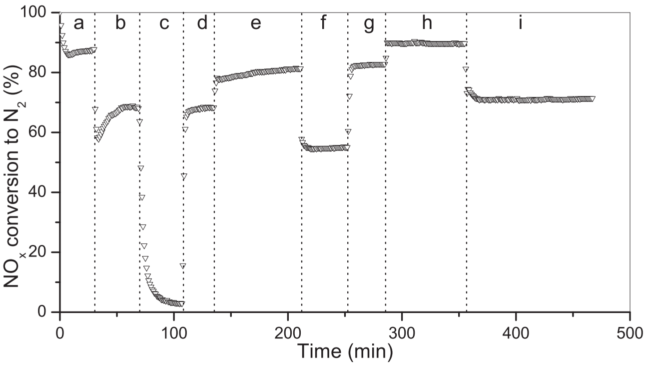

Fig. 3. Transient response results for feeding 3% H_2O (when used), 5% O_2, 500 ppm NH_3, 450 ppm NO_x, 72,000 L/(kg h), 250 °C: (a) NO = 450 ppm without H_2O; (b) add H_2O; (c) remove O_2; (d) add O_2; (e) NO=NO_2 = 225 ppm; (f) remove O_2; (g) add O_2; (h) NO_2 = 450 ppm; (i) remove O_2.

Based on our previous research [23], the reactions are shown below:

During the NO_2 adsorption step,

$$NO_2 + {-C(*)} \rightarrow {-C(NO_2)} \tag{4}$$

$$-C(NO_2) \rightarrow -C(O) + NO \tag{5}$$

$$-C(O) + NO_2 \rightarrow -C(ONO_2) \tag{6}$$

During the TPD step

$$-C(ONO_2) \rightarrow -C(O) + NO_2 \quad \sim 130\,^{\circ}C \tag{7}$$

$$-C(ONO_2) \rightarrow -C(O_2) + NO \quad > 130\,^{\circ}C \tag{8}$$

The formation of CO_2 and CO is attributed to the following reactions:

$$2C{-}C(O) \rightarrow C{-}C(*) + CO_2 + {-C(*)} \tag{9}$$

$$C{-}C(O) \rightarrow CO + {-C(*)} \tag{10}$$

$$C{-}C(O_2) \rightarrow CO_2 + {-C(*)} \tag{11}$$

where –C(*) denotes an active site and $-C(O_2)$ represents a surface complex comprising two oxygen atoms.

3.2. Transient response results

The NO_x conversion to N_2 became stable after 10 min as shown in Fig. 3, and the main reaction is the “standard SCR” reaction at this time. On adding 3% H_2O into the feed stream after 30 min, the NO_x conversion to N_2 decreased sharply and reached a steady-state of about 70%. This result is ascribed to H_2O inhibiting the SCR reaction, which is between the NH_3 adsorbed on the Lewis acid sites of the V_2O_5/AC catalyst and NO, as reported by Huang et al. [26]. In step (c), O_2 addition to the feed gas was terminated and a drastic

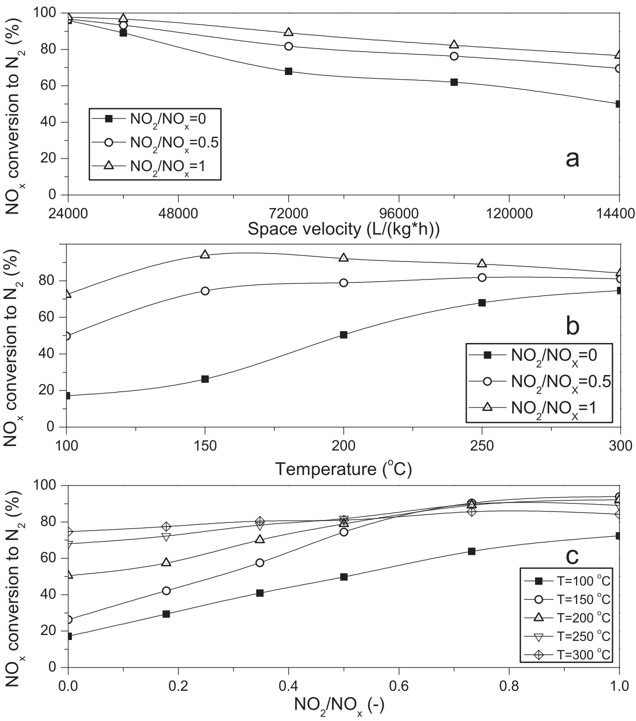

Fig. 4. NO$_x$ conversion to N$_2$ as function of space velocity, temperature and NO$_2$/NO$_x$ ratio for 450 ppm NO$_x$, 500 ppm NH$_3$, 5% O$_2$, 3% H$_2$O, 250 °C for (a), 72,000 L/(kg h) for (b and c).

drop in NO$_x$ conversion to N$_2$ was observed. This is attributed to the need for oxygen in "standard SCR" to reoxidize the reduced catalyst, which is the rate-determining step of the overall reaction according to the mechanism investigated by Lietti and Forzatti [27]. The slow decrease in NO$_x$ conversion to N$_2$ is due to the ability of the lattice oxygen and surface oxygen functionalities on the catalyst to participate in the reaction between NO and NH$_3$ in the absence of O$_2$ [28,29]. The remaining 3% of the NO$_x$ conversion to N$_2$ is ascribed to the following reaction:

$$4NH_3+6NO \rightarrow 5N_2+6H_2O \qquad (12)$$

When O$_2$ was supplied again at 110 min, NO$_x$ conversion to N$_2$ immediately increased and reached the original level. In step (e), NO$_x$ conversion to N$_2$ increased to 81% when a 0.5 NO$_2$/NO$_x$ ratio was fed. Oxygen dosing was then stopped again after 210 min. Unlike step (c), NO$_x$ conversion to N$_2$ decreased and became stable at 57% rapidly, indicating the effect of NO$_2$ on the reaction. It was reported that both NO$_2$ and HNO$_3$ are able to reoxidize the vanadium catalyst at a much lower temperature than gaseous O$_2$ [18,19]. The NO$_x$ conversion to N$_2$ then recovered to the step (e) profile after oxygen was supplied again at 255 min. In step (h), the NO$_2$/NO$_x$ ratio was switched to 1 and NO$_x$ conversion to N$_2$ increased to 90%. Oxygen dosing was stopped again after 355 min, and NO$_x$ conversion to N$_2$ became stable rapidly.

The ratio of consumed NH$_3$ to NO$_x$ is maintained at nearly 1 throughout the process, indicating that the following reaction does not occur when NO$_2$ is added into the feed gas.

$$8NH_3+6NO_2 \rightarrow 7N_2+12H_2O \qquad (13)$$

3.3. The SCR activity

Fig. 4a shows the effect of space velocity on NO$_x$ conversion to N$_2$ with three different NO$_2$/NO$_x$ ratios at 250 °C. For a space velocity of 24,000 L/(kg h), nearly 100% NO$_x$ conversion to N$_2$ was achieved whether NO$_2$ existed or not. It then decreased with increasing space velocity up to 144,000 L/(kg h). This decrease slowed with increasing the NO$_2$/NO$_x$ ratio, confirming the promoting effect of NO$_2$. These results demonstrate that the V$_2$O$_5$/AC catalyst is highly effective for NO$_x$ conversion to N$_2$ within a wide range of space velocity, especially when replacing NO with NO$_2$. The N$_2$O formation did not exceed 10 ppm in any of the experiments, suggesting that an effective selectivity can be achieved.

As illustrated in Fig. 4b, NO$_x$ conversion to N$_2$ increased at NO$_2$/NO$_x$ = 0 when the temperature was increased from 100 to 300 °C. This result reveals that the "standard SCR" is enhanced with increasing temperature on the V$_2$O$_5$/AC catalyst. However, the NO$_2$-SCR was reduced with increasing temperature because of the conversion of NO$_2$ to NO on the catalyst, as shown in Fig. 1. When NO was replaced with NO$_2$, the NO$_x$ conversion to N$_2$ increased slightly with temperature from 150 to 300 °C at NO$_2$/NO$_x$ = 0.5. For a ratio of 1, NO$_x$ conversion reached its maximum at 150 °C and then gradually decreased. Consequently, the application of NO$_2$-SCR on a V$_2$O$_5$/AC catalyst must be carried out at low temperatures.

It was reported that the optimum NO$_2$/NO$_x$ ratio of the SCR reaction is 0.5 for the catalysts such as V$_2$O$_5$–WO$_3$–MnO$_2$/TiO$_2$ and Fe-ZSM5, NO$_x$ conversion to N$_2$ then decreases with increasing the NO$_2$/NO$_x$ ratio due to the low reaction rate of the "NO$_2$ reaction" [14,15]. However, NO$_x$ conversion to N$_2$ on V$_2$O$_5$/AC catalyst increased significantly with increasing the NO$_2$/NO$_x$ ratio from 0 to 1 at low temperatures as shown in Fig. 4c. An increase of NO$_x$ conversion to N$_2$ form 26% to 94% was achieved at a temperature as low as 150 °C.

The increase of NO$_x$ conversion to N$_2$ then vanished gradually as the temperature increased from 150 °C to 300 °C. A possible explanation for this result can be associated with the conversion of NO$_2$ to NO as discussed above, which is enhanced by increasing temperature. The NO$_2$-SCR reaction is weakened at high temperatures due to the increase of the NO$_2$ conversion to NO. It is evidently observed that the concentrations of the effluent CO$_2$ and CO increased with increasing temperature or the NO$_2$/NO$_x$ ratio in the experiments, as shown in Fig. 5.

3.4. NH$_4$NO$_3$ formation and decomposition

As a critical issue for the application of a catalyst in NO$_2$-SCR system, a series of experiments were carried out to investigate the formation and decomposition of NH$_4$NO$_3$ on the catalyst. Fig. 6 shows the results of NH$_4$NO$_3$-TPD. Marked increases in NO and CO$_2$ concentrations were observed first, indicating the adsorption and conversion of NO$_2$ to NO. The NH$_3$ concentration broke through after 6 min, which is attributed to the ability of the catalyst to adsorb NH$_3$ [30]. The outlet NO then decreased because of the SCR reaction involving NH$_3$, NO and O$_2$. The outlet concentrations of NO and NH$_3$ reached the steady-state simultaneously. The values suggest that the consumption ratio of NO$_2$ and NH$_3$ is still close to 1.

A sharp desorption of NH$_3$ was observed first when a subsequent TPD experiment run at 10 °C/min was performed. The emission of NO, N$_2$O, CO, and CO$_2$ became significant with increasing temperature, confirming the deposition of NH$_4$NO$_3$ in the NO$_2$ conversion step. There was no detectable amount of NO$_2$ observed in the efflux. The desorption peaks corresponding to various gases occurred simultaneously around 130 °C, which coincide with the NO$_2$ desorption peak shown in Fig. 2a. This decomposition temperature is significantly lower than the corresponding temperature of the deposited NH$_4$NO$_3$ over other catalysts, which is 170 °C [17,31].

In summary, all of the observed products in the TPD results such as NH$_3$, NO, CO$_2$, CO, and N$_2$O can be associated with a series of reactions as follows:

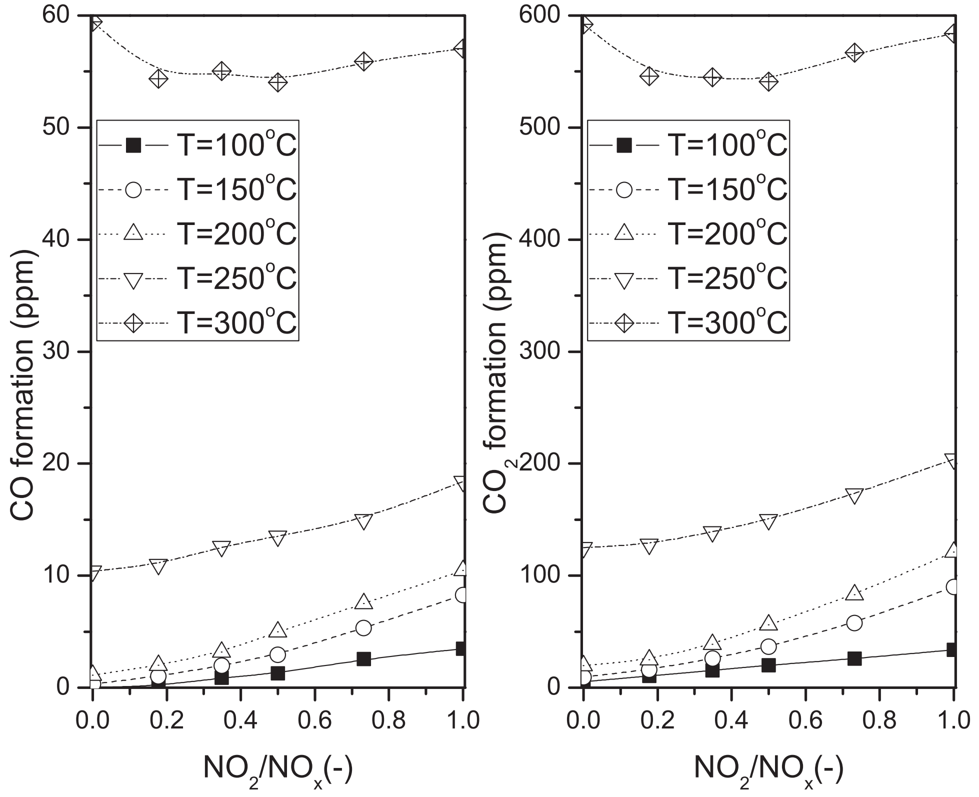

Fig. 5. CO and CO_2 formation during the SCR activity tests.

(i) Desorption of the adsorbed NH_3.

(ii) The decomposition of NH_4NO_3 according to the following stoichiometry:

$$NH_4NO_3 \leftrightarrow NH_3 + HNO_3 \tag{14}$$

(iii) Reaction between AC and HNO_3. It was reported that HNO_3 is a much better oxidizing agent than NO_2, and the reaction between AC and HNO_3 can produce nitrogen and oxygen complexes on the catalyst [25,32].

$$-C(*) + HNO_3 \rightarrow -C(O) + HNO_2 \tag{15}$$

$$-C(O) + HNO_2 \rightarrow -COOH + NO \tag{16}$$

$$2{-}C(*) + 2HNO_2 \rightarrow N2O + H2O + 2{-}C(O) \tag{17}$$

(iv) The decomposition of the oxygen complexes according to reactions (9)–(11).

The reactions (15) and (16) easily occur at very low temperatures, as observed in the treatment of AC using nitric acid [33]. It is why NO desorption peak is around 130 °C. Moreover, the oxidation with HNO_3 leads to carbons with a predominant population of surface carboxylic groups (-COOH), which decompose at low temperatures [34,20]. It accounts for a large amount of CO and CO_2 appears in the efflux during the TPD step, which is different from that in Fig. 2. The emission of N_2O around 130 °C indicates that the decomposition of NH_4NO_3 yielding N_2O and H_2O is not reasonable due to the higher temperatures needed. Accordingly,

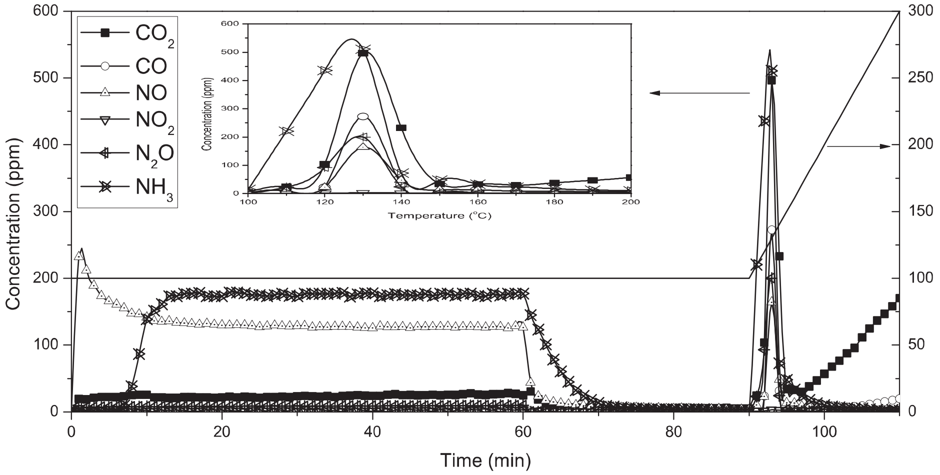

Fig. 6. Outlet concentrations of CO_2, CO, NO, NO_2, N_2O, and NH_3 vs. time. Before 60 min: NO_2 conversion step for 450 ppm NO_2, 500 ppm NH_3, 5% O_2, 3% H_2O, 100 °C, 72,000 L/(kg h). After 60 min: purge + TPD step under exposure to Ar.

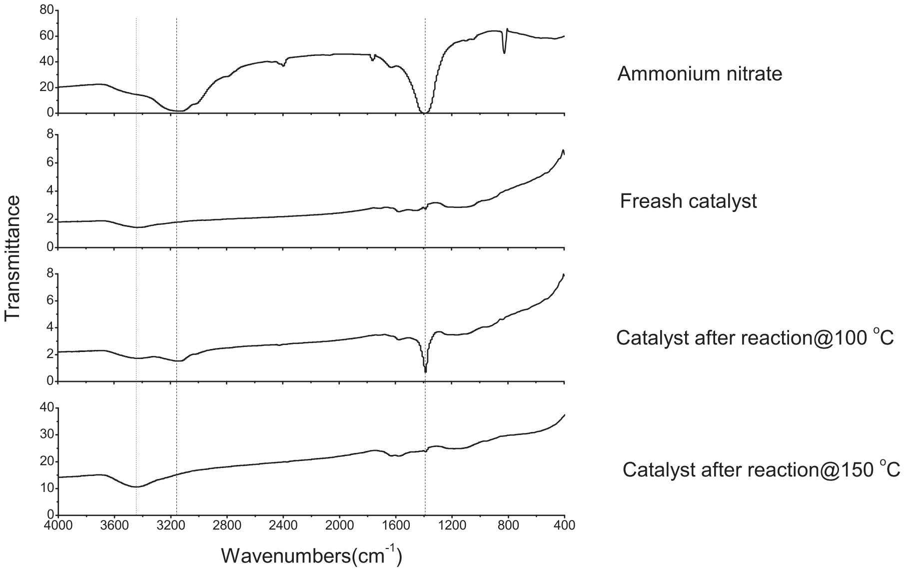

Fig. 7. IR spectra of commercial NH_4NO_3, fresh V_2O_5/AC catalyst and catalyst after reaction at 100 and 150 °C for 5 h using 900 ppm NO_2, 1000 ppm NH_3, 5% O_2, 3% H_2O, 72,000 L/(kg h).

reaction (17) may be a reasonable explanation to the formation of nitrous oxide. Due to the participation of AC, the conversion temperature of NH_4NO_3 is significantly reduced, even below its melting temperature.

A similar experiment, using the same feed mixture and procedure, was performed at 150 °C for comparison. The results show that just a small amount of NH_3 desorbs in the TPD step. This is in agreement with the desorption peaks at 130 °C shown in Fig. 6, demonstrating that NH_4NO_3 is not deposited at 150 °C.

IR analyses were carried in order to clarify the deposition of the NH_4NO_3 on the catalyst. As shown in Fig. 7, the catalyst after reaction at 100 °C exhibits the two IR bands characteristic for NH_4NO_3 (1380 and 3150 cm^{-1}) [31]. However, the catalyst after reaction at 150 °C exhibits almost no differences from the spectrum for the fresh catalyst, confirming that there is no NH_4NO_3 deposition on the catalyst at this temperature.

3.5. Role of AC support in NH_3–NO/NO_2-SCR

During the SCR activity tests, maximum deNO$_x$ activity, achieved at NO_2/NO_x feed ratio of 1/1 instead of 1/2, was observed. This can be ascribed to the participation of AC support. In the presence of NO_2, the reaction (18) occurs. However, the ammonium nitrate formed has to be cleared up further [17]. For fast SCR, the conversion of NH_4NO_3 depends on its subsequent reduction by NO based on reaction (19). Accordingly, Nova et al. suggested an alternative sequential scheme, whereby the fast SCR reaction (2) results from the formation of NH_4NO_3, reaction (18), and its reduction by NO, reaction (19) [35].

$$2NH_3+2NO_2 \rightarrow N_2+NH_4NO_3+H_2O \tag{18}$$

$$NO+NH_4NO_3 \rightarrow N_2+NO_2+2H_2O \tag{19}$$

At low temperature the fast SCR is limited by the reaction between NH_4NO_3 and NO. For AC involved NO_2-SCR, the conversion of NH_4NO_3 depends on reactions (14), (15) and the following reaction (20).

$$NH_4NO_3 \leftrightarrow NH_3+HNO_3$$

$$-C(*)+HNO_3 \rightarrow -C(O)+HNO_2$$

$$HNO_2+NH_3 \rightarrow [NH_4NO_2] \rightarrow N_2+2H_2O \tag{20}$$

$$\overline{NH_4NO_3+-C(*) \rightarrow -C(O)+N_2+2H_2O} \tag{21}$$

Considering the consecutive steps, we obtain an overall stoichiometry which roughly reflects the reduction of NH_4NO_3 by AC instead of NO. From the NH_4NO_3-TPD results, it is reasonable to conclude that compared with fast SCR, AC involved NO_2-SCR has better reactivity at lower temperatures. Meanwhile, due to the excess NH_3 in the gas phase and over the catalyst surface, the reactions (16) and (17) are inhibited and reaction (20) is preferred.

Due to the reaction (5) in parallel to SCR reaction (see Fig. 1) and the oxidation of reduced vanadium species by NO_2 to keep the activity (see Fig. 3 step (i)), the introduction of NO into the reacting system is inevitable. The NO removal according to fast SCR needs higher temperatures and rigorous stoichiometry, which are hard to be satisfied. More NO would result in the decrease of NO_x conversion, especially at 150 °C.

It is worth emphasizing that the NO_x conversion to N_2 increased from 26% at $NO_2/NO_x = 0$ to 75% at $NO_2/NO_x = 0.5$ for the temperature of 150 °C. This increase would be more significant at a lower space velocity. Even if 100% conversion of NO to NO_2 is hard to reach under actual conditions by the NTP catalytic process and the oxidation catalyst [12,13], the largest increase of NO_x conversion to N_2 at 150 °C suggests that the conversion of a fraction of NO to NO_2 is still significant to get high NO_x removal efficiency at low temperatures.

During the AC involved NO_2-SCR process, the active sites of carbon (–C(*)) gradually decrease. The catalyst needs thermal treatment to recover the active sites. Our previous research verified that little change of AC performance was observed with increasing the thermal treatment times [23]. Moreover, we just reported a similar V_2O_5/AC catalyst shows the good performance of SO_2 removal at 150 °C [36]. Combined with the NTP process, the simultaneous removal of SO_2 and NO using the V_2O_5/AC catalyst at low temperature seems an alternative to the current SCR and wet flue gas desulfurization (WFGD) system.

4. Conclusions

The V_2O_5/AC catalyst exhibits high activity and selectivity in the SCR reaction with feed gas containing both NO and NO_2. With the conversion to NO, NO_2 is adsorbed on the catalyst. The NO_x conversion to N_2 increases with increasing NO_2/NO_x ratio at low temperature, in which the largest increase occurs at 150 °C. The increase slows with increasing temperature because of the conversion of NO_2 to NO. NH_4NO_3 tends to be deposited on the catalyst at 100 °C and can be decomposed to NH_3, N_2O, and NO around 130 °C, confirming that the NO_x removal at 150 °C is effective without the formation of NH_4NO_3. AC involved NO_2-SCR process was proposed to explain the observed behaviors. In this process, NH_4NO_3 is reduced to N_2 by AC instead of NO, which has better reactivity at lower temperatures.

Acknowledgements

We gratefully acknowledge the financial support of the National Natural Science Foundation of China (No. 50776079) and Development of China (863 Program) (No. 2007AA061802).

References

[1] H.E. Curryhyde, H. Musch, A. Baiker, Appl. Catal. B: Environ. 65 (1990) 211–223.
[2] M. Kang, D.J. Kim, E.D. Park, J.M. Kim, J.E. Yie, S.H. Kim, L. Hope-Weeks, E.A. Eyring, Appl. Catal. B: Environ. 68 (2006) 21–27.
[3] X. Gao, Y. Jiang, Y. Zhong, Z.Y. Luo, K.F. Cen, J. Hazard. Mater. 174 (2010) 734–739.
[4] L. Chen, J.H. Li, M.F. Ge, J. Phys. Chem. C 113 (2009) 21177–21184.
[5] L. Chen, J.H. Li, M.F. Ge, Environ. Sci. Technol. 44 (2010) 9590–9596.
[6] P.A. Kumar, M.P. Reddy, L.K. Ju, B. Hyun-Sook, H.H. Phil, J. Mol. Catal. A: Chem. 291 (2008) 66–74.
[7] Z.B. Wu, R.B. Jin, Y. Liu, H.Q. Wang, Catal. Commun. 9 (2008) 2217–2220.
[8] Z.P. Zhu, Z.Y. Liu, S.J. Liu, H.X. Niu, Appl. Catal. B: Environ. 23 (1999) L229–L233.
[9] X.L. Tang, J.M. Hao, W.G. Xu, J.H. Li, Catal. Commun. 8 (2007) 329–334.
[10] J.H. Li, J.J. Chen, R. Ke, C.K. Luo, J.M. Hao, Catal. Commun. 8 (2007) 1896–1900.
[11] A. Kato, S. Matsuda, F. Nakajima, M. Imanari, Y. Watanabe, J. Phys. Chem. 85 (1981) 1710–1713.
[12] M.F. Irfan, J.H. Goo, S.D. Kim, Appl. Catal. B: Environ. 78 (2008) 267–274.
[13] Z.L. Wu, X. Gao, Z.Y. Luo, E.Z. Wei, Y.S. Zhang, J.Z. Zhang, M.J. Ni, K.F. Cen, Energy Fuels 19 (2005) 2279–2286.
[14] J.H. Goo, M.F. Irfan, S.D. Kim, S.C. Hong, Chemosphere 67 (2007) 718–723.
[15] M. Devadas, O. Krocher, M. Elsener, A. Wokaun, N. Soger, M. Pfeifer, Y. Demel, L. Mussmann, Appl. Catal. B: Environ. 67 (2006) 187–196.
[16] J. Blanco, P. Avila, S. Suarez, J.A. Martin, C. Knapp, Appl. Catal. B: Environ. 28 (2000) 235–244.
[17] M. Koebel, M. Elsener, G. Madia, Ind. Eng. Chem. Res. 40 (2001) 52–59.
[18] E. Tronconi, I. Nova, C. Ciardelli, D. Chatterjee, M. Weibel, J. Catal. 245 (2007) 1–10.
[19] X. Gao, X.S. Du, Y. Jiang, Y. Zhang, Z.Y. Luo, K.F. Cen, J. Mol. Catal. A: Chem. 317 (2010) 46–53.
[20] K. Kante, E. Deliyanni, T.J. Bandosz, J. Hazard. Mater. 165 (2009) 704–713.
[21] N. Shirahama, S.H. Moon, K.H. Choi, T. Enjoji, S. Kawano, Y. Korai, M. Tanoura, I. Mochida, Carbon 40 (2002) 2605–2611.
[22] M. Jeguirim, V. Tschamber, J.F. Brilhac, P. Ehrburger, J. Anal. Appl. Pyrolysis 72 (2004) 171–181.
[23] X. Gao, S.J. Liu, Y. Zhang, Z.Y. Luo, N.M. Jiang, K.F. Cen, Fuel Process. Technol. 92 (2011) 139–146.
[24] W.J. Zhang, A. Bagreev, F. Rasouli, Ind. Eng. Chem. Res. 47 (2008) 4358–4362.
[25] A. Jeguirim, V. Tschamber, J.F. Brilhac, P. Ehrburger, Fuel 84 (2005) 1949–1956.
[26] Z.G. Huang, Z.Y. Liu, X.L. Zhang, Q.Y. Liu, Appl. Catal. B: Environ. 63 (2006) 260–265.
[27] L. Lietti, P. Forzatti, J. Catal. 147 (1994) 241–249.
[28] E. Ito, R.J. Hultermans, P.M. Lugt, M.H.W. Burgers, M.S. Rigutto, H. Vanbekkum, C.M. Vandenbleek, Appl. Catal. B: Environ. 4 (1994) 95–104.
[29] M.E. Galvez, A. Boyano, M.J. Lazaro, R. Moliner, Chem. Eng. J. 144 (2008) 10–20.
[30] Z.P. Zhu, Z.Y. Liu, H.X. Niu, S.J. Liu, T.D. Hu, T. Liu, Y.N. Xie, J. Catal. 197 (2001) 6–16.
[31] C. Ciardelli, I. Nova, E. Tronconi, D. Chatterjee, B. Bandl-Konrad, M. Weibel, B. Krutzsch, Appl. Catal. B: Environ. 70 (2007) 80–90.
[32] S. Bashkova, T.J. Bandosz, J. Colloid Interface Sci. 333 (2009) 97–103.
[33] C. Moreno-Castilla, F. Carrasco-Marín, F.J. Maldonado-Hódar, J. Rivera-Utrilla, Carbon 36 (1997) 145–151.
[34] I. Salame, T.J. Bandosz, J. Colloid Interface Sci. 240 (2001) 252–258.
[35] I. Nova, C. Ciardelli, E. Tronconi, D. Chatterjee, B. Bandl-Konrad, Catal. Today 114 (2006) 3–12.
[36] X. Gao, S.J. Liu, Y. Zhang, Z.Y. Luo, K.F. Cen, J. Hazard. Mater. 188 (2011) 58–66.